Pergamon

Geochimica et Cosmochimica Acta, Vol. 65, No. 24, pp. 4539–4549, 2001

0016-7037/01 $20.00 + .00

PII S0016-7037(01)00738-4

^{16}O-rich melilite in CO3.0 chondrites: Possible formation of common, ^{16}O-poor melilite by aqueous alteration

JOHN T. WASSON,[1,*] HISAYOSHI YURIMOTO,[2] and SARA S. RUSSELL[3]

[1]Institute of Geophysics and Planetary Physics, University of California, Los Angeles, CA 90095-1567, USA
[2]Department of Earth and Planetary Sciences, Tokyo Institute of Technology, Ookayama, Meguro, Tokyo 152-8551, Japan
[3]Department of Mineralogy, The Natural History Museum, Cromwell Road, London, SW7 5BD, United Kingdom

(*Received August* 15, 2000; *accepted in revised form April* 20, 2000)

Abstract—A problem of long-standing is the origin of the high $\Delta^{17}O$ ($= \delta^{17}O - 0.52 \cdot \delta^{18}O$) values of melilite in the refractory inclusions of carbonaceous chondrites. The spinel and, usually, also the diopside in the inclusions have "primitive" $\Delta^{17}O \leq -20‰$, but in the widely studied CV3 chondrite Allende, the melilite commonly has a $\Delta^{17}O$ of about $-4 \pm 2‰$. Recent studies of oxygen diffusion coefficients in melilite and spinel have shown that the traditional model for altering the melilite—diffusive exchange with the gas in the solar nebula—cannot occur under plausible nebular scenarios. Because of increasing evidence for aqueous alteration of Allende and other carbonaceous chondrites, we tested the hypothesis that melilite alteration might occur during aqueous alteration by studying melilite in CO chondrites showing variable degrees of alteration. Our results show that almost all melilite in CO3.2 Kainsaz and CO3.3 Ornans has $\Delta^{17}O > -15‰$, whereas in CO3.0 Colony (and inclusions in CO3.0 Yamato 81020 studied by Itoh et al. [2000]) $\Delta^{17}O$ in the melilite is $< -20‰$ (with the exception of one unusual inclusion that has undergone two melting episodes). We suggest that the O-isotopic composition of the melilite is reset by dissolution of the primitive melilite and reprecipitation in the presence of H_2O having a high $\Delta^{17}O$ value similar to that inferred from studies of CV magnetite (Choi et al., 1997, 2000). Although alteration of melilite can produce phases such as nepheline, andradite, and hedenbergite, it appears that, depending on the composition of the microenvironment, melilite present in a high-energy state (because of fine grain size, dislocations, other defects) can dissolve and reprecipitate with an O-isotopic composition intermediate between the initial composition and that of the H_2O. A possible implication of our study is that the slope ≈ 0.9 arrays observed in the minerals of refractory inclusions of many carbonaceous chondrites could be mainly the result of aqueous alteration.

1. INTRODUCTION

The discovery that the O-isotopic composition of most meteorites and their constituent phases do not plot along the slope-1/2 terrestrial fractionation (TF) line (Clayton et al., 1973, 1977, 1991) has provided strong evidence that, at different times or places, the solid materials agglomerated from the solar nebula had diverse origins. The simplest model is that the presolar material from which the solar nebula formed was heterogeneous, and each batch of matter accreting to the nebula consisted of a different mix of ejecta from a variety of stars (e.g., Wasson, 2000).

Many of the initial studies were from the Allende CV3 carbonaceous chondrite. Particularly deviant from the TF line were spinel, diopside, and some other minerals in the refractory inclusions (commonly called calcium-aluminum-rich inclusions or CAIs) which, with rare exceptions, plotted around $\delta^{17}O = -41‰$, $\delta^{18}O = -40‰$ (relative to the SMOW standard). A convenient measure of the deviation from the TF line is $\Delta^{17}O = (\delta^{17}O - 0.52 \cdot \delta^{18}O)$, thus typical refractory inclusions contain some minerals with $\Delta^{17}O$ values of $-20‰$ or lower. For convenience in the following discussion of the minerals of refractory inclusions, we refer to O-isotopic compositions having $\Delta^{17}O$ values of $-20‰$ or lower as "primitive."

* Author to whom correspondence should be addressed (jtwasson@ucla.edu).

An early surprise concerned the O-isotopic heterogeneity of refractory inclusions in CV Allende. Clayton et al. (1977) observed that mineral phases and mixtures of phases separated from coarse-grained refractory inclusions formed an array designated the carbonaceous-chondrite-anhydrous minerals (CCAM) line; the slope of the array is ≈ 0.94, and it extends from the above CAI composition to an intersection with the TF line at about $\delta^{18}O = +9‰$. It is common practice to include the CCAM reference line on plots of $\delta^{17}O$ vs. $\delta^{18}O$. In this article, we focus the discussion on melilite and spinel, but it should be noted that data by Clayton and coworkers show that one other relatively common phase, anorthite, tends to be similar in $\Delta^{17}O$ to melilite and that pyroxene tends to be similar to (but generally slightly less negative than) spinel.

Even though melilite can form as a refractory condensate (or evaporation residue) in a canonical (solar-composition) nebula (Grossman, 1972) and is also one of the first phases to crystallize from a cooling melt of refractory oxides (Stolper and Paque, 1986), Clayton et al. (1977) found that the typical composition of melilite from coarse-grained CAIs in Allende is $\delta^{18}O = -1 \pm 3‰$, $\Delta^{17}O = -4 \pm 2‰$. In Figure 1, we plot data for phases separated from type-B several Allende inclusions by Clayton et al. (1977) and Mayeda et al. (1986).

Clayton et al. (1977; Clayton and Mayeda, 1984) examined several models to account for the deviation of the melilite composition from the $\Delta^{17}O$ value of $-20‰$ that was inferred to have been present initially. They concluded that the most

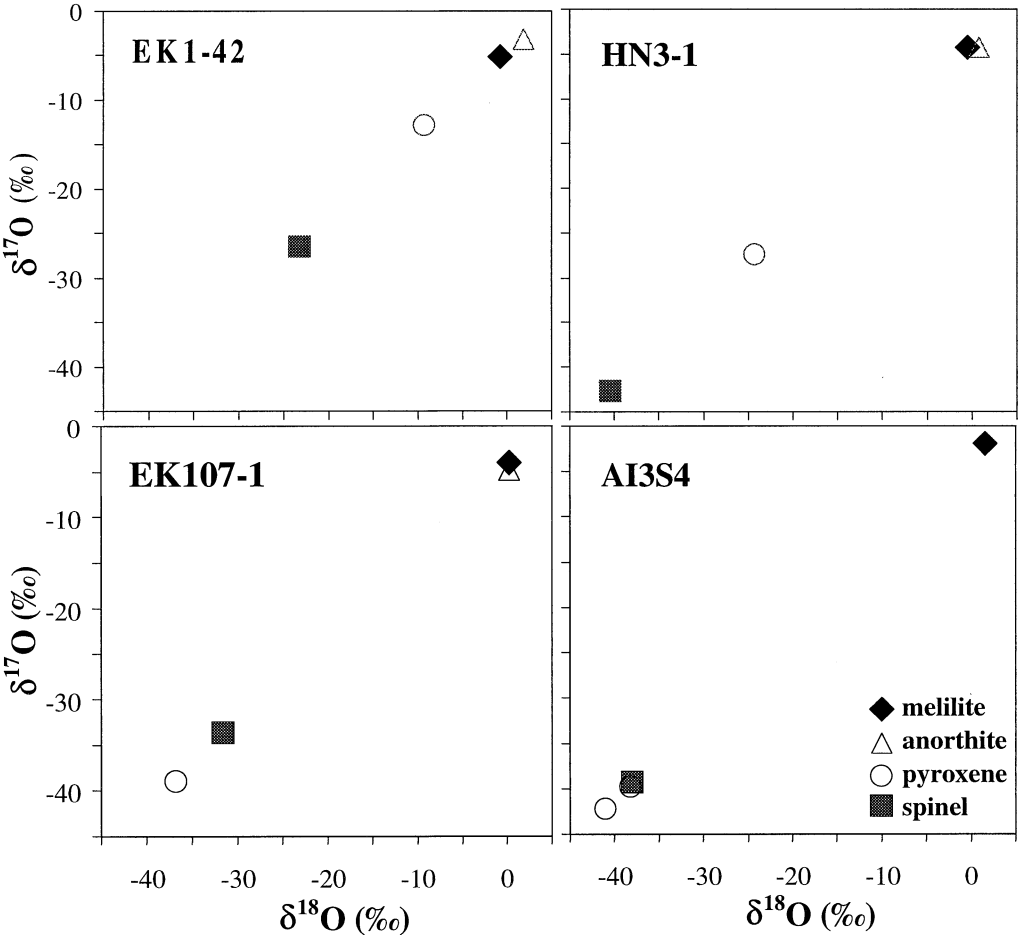

Fig. 1. O-isotopic compositions of phases from type-B coarse-grained refractory inclusions from CV Allende; Hand-picked samples of EK1-42. EK107-1 and HN3-1 analyzed by Mayeda et al. (1986) and density separates of Al3S4 studied by Clayton et al. (1977). The "pyroxene" analyzed in Al3S4 included a minor fraction of spinel.

plausible model was one in which the solid melilite exchanged oxygen with a high $\Delta^{17}O$ nebula gas (Blander and Fuchs, 1975; Chou et al., 1976), the melilite undergoing much more exchange than the spinel because O diffused more rapidly in it than in spinel.

At the time this interpretation was offered, there were no high-quality diffusion data for melilite or spinel. When this deficiency was removed by the detailed studies of Yurimoto et al. (1989) and Ryerson and McKeegan (1994), it was found that the diffusion coefficient of O in melilite was indeed greater than that in spinel but, more important, that no plausible nebular scenario involving solid state diffusion or diffusion into a crystallizing melt during simple cooling scenarios could account for the O-isotope distribution among phases (Fig. 1) observed in the studies of Clayton et al. (1977). Diffusion times are much too long. Ryerson and McKeegan (1994) calculated that it would take 1 to 10 yr to equilibrate a 1-mm grain at 1670 K, around the solidus temperature of melilite. At a temperature of 1470 K, below the solidus, it would take ~10 times longer to equilibrate. Temperatures must drop to ≈1250 K for forsterite to condense, but the forsterite associated with refractory inclusions that have escaped aqueous alteration tends to have $\Delta^{17}O$ near or below −20‰ (Hiyagon and Hashimoto, 1999; Sakai and Yurimoto, 1999). And, if there was a temperature gradient between the midplane and surface of an opaque nebula (Cassen, 1996), it is unlikely that temperatures of the inclusions could have remained roughly constant for a 10- to 100-yr period. In an attempt to deal with these difficulties, Yurimoto et al. (1998) proposed a multistage melting model for the origin of coarse-grained igneous CAIs.

During the last several years, the evidence for aqueous alteration of carbonaceous chondrites has accumulated at a high rate. Kojima et al. (1995) and Krot et al. (1995) listed several criteria that indicated that carbonaceous chondrites had experienced moderate amounts of aqueous alteration including the formation of magnetite by corrosion of metal, the formation of phyllosilicates, and the replacement of melilite by nepheline, sodalite, hedenbergite, and andradite. Blum et al. (1989) had already concluded that such low-temperature processes offered the best explanation for the strange metal-sulfide ("opaque") assemblages found in some Allende refractory inclusions. Some alteration features in coarse-grained (type-B) inclusions in Allende were recognized by Meeker et al. (1983) and attributed to metamorphic reactions, possibly with a fluid phase.

Given the evidence that so many phases have experienced alteration, we hypothesized that the position of typical CV

melilite high on the CCAM line might be the result of aqueous alteration. Replacement of a preexisting phase in the presence of moisture might offer the possibility of large-scale exchange of O in a way that avoided the need for volume diffusion within solid phases.

Kojima et al. (1995), and Shibata (1996) surveyed the petrographic characteristics of CO chondrites and found evidence interpreted to indicate that the petrologic subtypes reflected increasing degrees of aqueous/metamorphic alteration from 3.0 (Colony, Yamato 81020 and Allan Hills ALHA77307) to 3.7 (Isna). Examination of the available evidence suggests that, on average, the CO chondrites have experienced less alteration than CV chondrites and that the CO3.0 chondrites might be among the least altered carbonaceous chondrites (e.g., Brearley et al., 1995). We therefore embarked on the present study of CO melilite with the thought that, if aqueous alteration played a role in resetting the isotopic composition of melilite, we would find that lower petrographic subtypes preserved a more primitive composition than the higher subtypes.

2. EXPERIMENTAL

2.1. Petrology

We studied three thin sections from the Natural History Museum, CO3.0 Colony (section S1361, 15 mm^2), CO3.2 Kainsaz (S1362, 150 mm^2), and CO3.3 Ornans (BM1985, M149, 220 mm^2). Back-scattered-electron (BSE) images of the entire carbon-coated sections were prepared using a scanning electron microscope. Refractory inclusions were located by X-ray mapping, and detailed BSE images prepared for the ion-probe studies. Elemental compositions were determined by using a Cameca SX50 wavelength dispersive electron microprobe at the Natural History Museum.

2.2. Ion-Probe Techniques

Oxygen isotopes were analyzed using the Cameca 1270 ion microprobe (IMP) at the Tokyo Institute of Technology. The primary ion beam was mass-filtered positive 20-keV Cs ions; the typical spot size was 4 μm. The primary beam current was $\approx$3 pA, adjusted to obtain a count rate of $\approx 4 \cdot 10^5$ cps for negative ^{16}O ions. A normal incidence electron gun was used for charge compensation. Negative secondary ions corresponding to the ^{16}O tail, ^{16}O, ^{17}O, ^{16}OH, and ^{18}O were analyzed at a mass resolution of $\approx$6000. Additional analytical procedures are described in Yurimoto et al. (1998).

3. RESULTS

3.1. Petrology

The petrologic subtypes of CO3 chondrites are not completely uncontentious. Part of the problem is that in this group the observed alteration is in part the result of aqueous processes and in part the result of thermal recrystallization and dehydration. There is a general agreement on petrologic grounds that Colony and Yamato 81020 are CO3.0 chondrites. Although Kallemeyn and Wasson (1982) inferred that Allan Hills ALHA77307 was not a CO chondrite but instead a close relative, mainly because its Cd concentration was well above the range defined by other CO chondrites, they could not completely rule out the possibility of Cd contamination. They also cited the higher matrix abundance and the higher Cr content of the metal in ALH77307, but these properties now appear consistent with a CO3.0 classification in light of more recent studies of the CO3.0 chondrites Colony (Rubin et al., 1985) and Yamato 81020 (e.g., Kojima et al., 1995; Shibata, 1996; Grossman and Rubin, 1999) that were not known at the time of the Wasson-Kallemeyn study. The current view of Wasson is that ALH77307 should be treated as a "normal" CO until evidence contrary to this assignment more compelling than the Cd concentration is found.

The subtype of Kainsaz also requires discussion. Scott and Jones (1990) described it as 3.1, whereas Sears et al. (1991) list it as a 3.3. Grossman and Rubin (1999) showed that it is much more altered than the type-3.0 CO chondrites; the degree of alteration seems too high to be characterized by a difference of only 0.1 in subtype. We tentatively list Kainsaz as CO3.2. The subtype of Ornans is 3.3 according to Scott and Jones (1990); 3.4 is according to Sears et al. (1991). We discuss below that based on the relatively primitive O-isotope data in some of its melilite, we find 3.3 to be more appropriate.

Inclusions bearing moderately large, clear melilite grains are relatively rare in our three sections of CO chondrites; we found only seven (one was accidentally destroyed) in a combined area of 390 mm^2. These inclusions—K1 and K2 (from Kainsaz); O3, O4, and O5 (from Ornans), and C1 (from Colony)—are shown in Figure 2. Detailed images of the analyzed spots are shown in Figures 3, 4, and 5. Phase compositions are listed in Table 1.

Kainsaz inclusion K1 is a more or less round, unrimmed, 200 $\times$ 250–μm inclusion (Fig. 2a). The core consists of melilite (Åk 3–7) enclosing perovskite and spinel (of variable composition; containing up to 12% FeO) grains. In the outer portion of the CAI ($\approx$60% of the total inclusion), the primary melilite has been altered to a submicron mix of nepheline, andradite, and hedenbergite. In this region, the alteration has destroyed much of the textural evidence regarding its formation. In the interior the intergrown grains and the relatively low porosity suggest that some melting preceded the final crystallization.

Kainsaz inclusion K2 is subrounded, 500 $\times$ 750–μm inclusion consisting of irregularly shaped, porous patches of melilite (Åk 14–28), spinel (0–5% FeO), and fine (micrometer-sized) perovskite (Fig. 2b). The melilite-rich areas are typically surrounded by a rim of anorthite, in turn surrounded by a thin alteration layer and an outer layer of Al-rich diopside (containing up to 2% TiO_2-Ti_2O_3 and 10% Al_2O_3). The porous texture of the inclusion combined with its layered structure suggests formation by condensation, but the interlocking grains also suggest that the CAI experienced a low degree of melting before final crystallization.

Ornans inclusion O3 is an irregularly shaped inclusion 180 μm across (Fig. 2c). It is predominantly composed of melilite (Åk9–12), enclosing micron to submicron grains of spinel and perovskite. The inclusion is rimmed by a $\sim$10-μm layer of Al-rich diopside, containing up to 6% Al_2O_3 and 1% TiO_2; the rim is zoned with the innermost part of the rim is richer in Al and Ti. Immediately inside the rim the CAI has been partly altered to submicrometer alteration products, probably composed of nepheline and FeO-rich pyroxenes.

Ornans inclusion O4 is an irregularly shaped, porous CAI 200 μm across in maximum dimension (Fig. 2d). It is composed of nodules of melilite (Åk10 to 18). Toward the edges of the inclusion patches of melilite associated with large pores have been altered to nepheline, andradite, and hedenbergite.

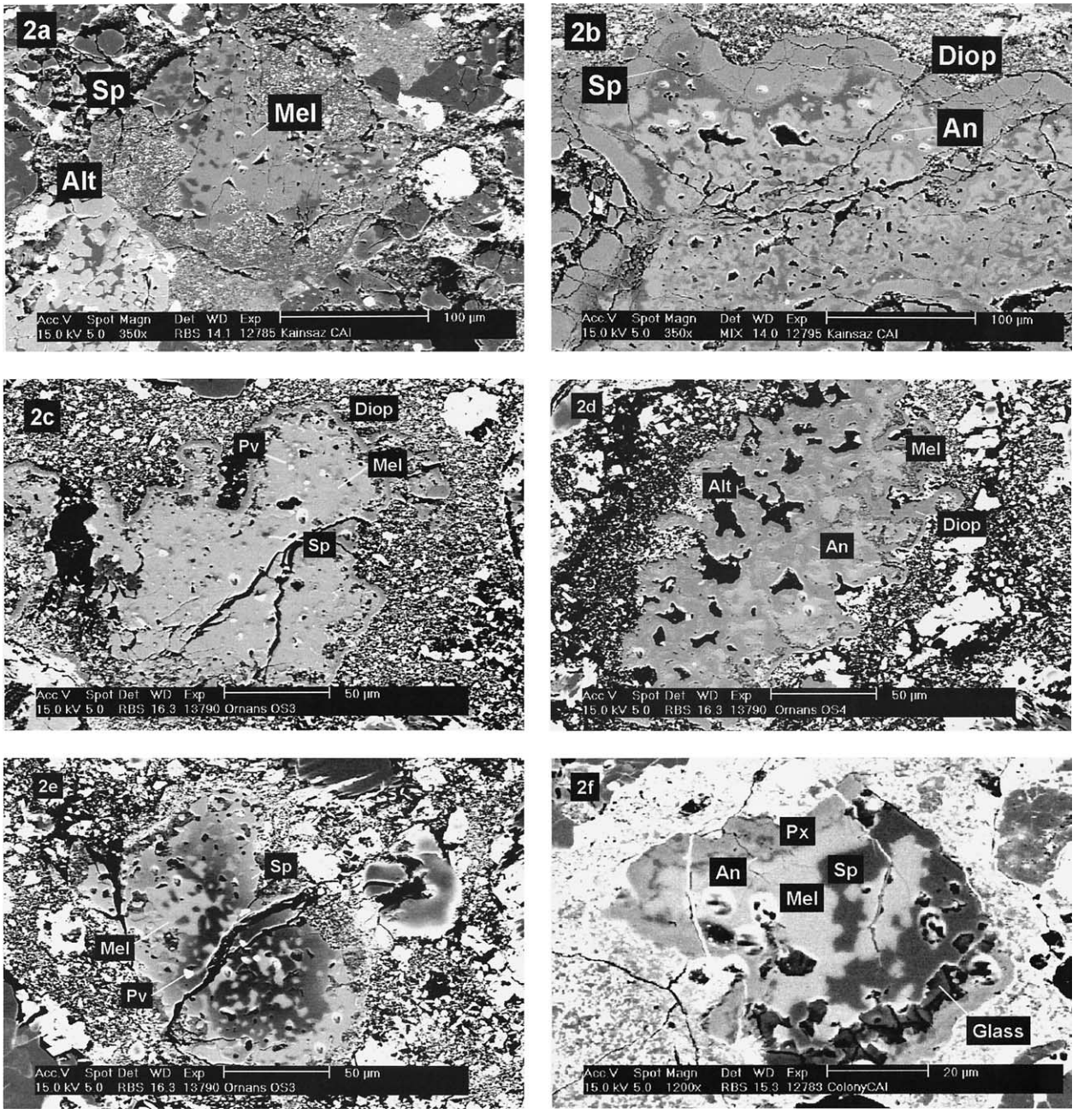

Fig. 2. Backscattered electron images of melilite-bearing inclusions from CO3 meteorites: Mel = melilite, Sp= spinel, Pv = perovskite, Diop=diopside, An = anorthite; Alt = regions altered to submicron mixes of Na-, Cl-, Fe–rich minerals. (a) Kainsaz K1, a rounded inclusion composed of a melilite-rich interior but extensively altered on the margins; see Figure 3. (b) A portion of Kainsaz K2, an irregularly shaped inclusion composed of melilite and spinel anorthite and diopside. (c) Ornans O3, a compact inclusion consisting mainly of melilite and containing numerous inclusions of spinel and perovskite. The inclusion has a thin rim of diopside. (d) Ornans O4, an irregularly shaped inclusion composed of melilite partially altered to Na-rich alteration products, and surrounded by a diopside rim. (e) Ornans O5, a compact, rounded inclusion composed of melilite, spinel highly zoned in Fe, and relatively large (~4-μm) inclusions of perovskite. (f) Colony C1 is a compact calcium-aluminum-rich fragment composed of melilite enclosing blocky spinel grains. It exhibits a complex rim, consisting of a thin layer of anorthite, surrounded by spinel; in one portion, there is an inner rim of Na-rich glass.

The melilite nodules are rimmed by submicron-sized beads of spinel, surrounded in turn by a ~5-μm layer of diopside.

Ornans inclusion O5 is a rounded, compact, unrimmed, fragmental, 130 × 80–μm CAI composed of melilite (Åk 1 to 9) intergrown with spinel of highly variable composition. Close to the edges of the inclusion, the spinel contains up to 20% FeO, and in the center as little as 3% FeO. Zoned spinel compositions are a common characteristic feature of spinel-melilite inclusions in Ornans (Russell et al., 1998). The inclusion contains perovskite crystals up to 4 μm across. (Fig. 2e).

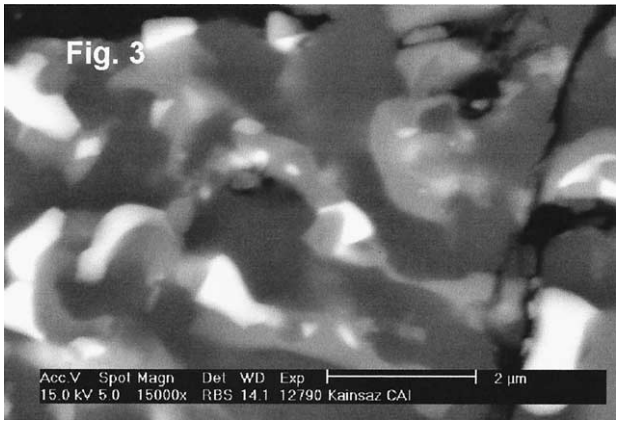

Fig. 3. Backscattered electron image of the altered region of Kainsaz K2. X-ray mapping and energy-dispersive X-ray analysis by scanning electron microscope revealed the mineralogy to be an intimate mixture of nepheline, diopside, sodalite, andradite, and hedenbergite.

The Cl content is high on the margins, possibly indicating the presence of fine sodalite.

Colony inclusion C1 is a compact, irregularly shaped, $\approx 30 \times 30 - \mu$m melilite-spinel inclusion that is incompletely rimmed (Fig. 2f) and thus appears to be a fragment. In the core of the inclusion the melilite (Ak1 to 29) encloses blocky spinel grains (FeO $<1\%$). The rim is composed of a thin anorthite layer surrounded by diopside; the diopside is zoned with Ti and Al increasing inward. The intergrown spinel and melilite, the relatively low porosity, and the irregular shape suggest crystallization from a mix containing a fraction of melt. The zoning of the diopside rim is consistent with outward growth. In melilite C1-01, some high FeO contents appeared to have been contaminated by adjacent weathering veins and were not included in the mean.

The primary mineralogy and bulk compositions of these three inclusions are typical for low petrologic type CO3 chondrites, but the large extent of alteration of K1 is unusual for a CO inclusion from petrologic subtype 3.2 (e.g., Russell et al., 1998).

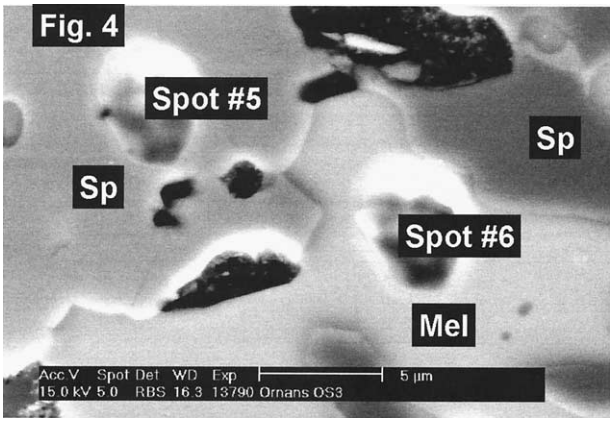

Fig. 4. Backscattered electron (BSE) image of ion microprobe pits in Ornans O5. Typical pit sizes are $\sim 5 \times 3$ μm. Note the heavily zoned spinel in this inclusion, indicated by the variation in BSE brightness. Mineral abbreviations as in Figure 2.

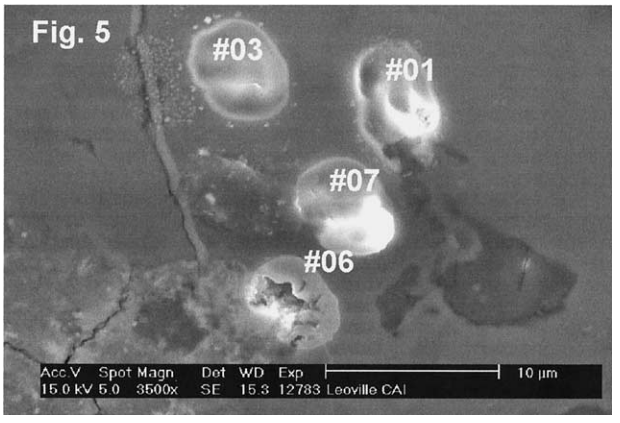

Fig. 5. Backscattered electron image of ion microprobe pits in Colony C1. Each of these pits are into melilite, with the exception of #06, which is a mixture of diopside and surrounding matrix.

3.2. Oxygen Isotopes

Our oxygen isotope data for phases in the six inclusions are listed in Tables 2 and 3 and plotted in Figure 6. The quoted uncertainties are 1 σ (mean); these are determined by counting statistics and replicate counts; typical values are ± 2‰ in δ^{18}O and ± 3‰ in δ^{17}O. We tested this generalization by assuming that the composition of the 6 points below -44, -44‰ in Kainsaz K2 (Fig. 6b) have identical compositions, and that the scatter is entirely experimental. Standard deviations for these 6 points are 2.8‰ for both δ^{18}O and δ^{17}O, consistent with the quoted uncertainties. The reproducibility of the standards is not included in these limits; if these it were included, it would increase the relative errors by $\sim 30\%$.

4. DISCUSSION

4.1. Original O-Isotopic Composition of CO Melilite

Our petrographic observations show extensive evidence of aqueous alteration in Kainsaz and Ornans, particularly in inclusion K1; we agree with others (e.g., Krot et al., 1995) that this alteration requires high H_2O activities only available in an asteroidal setting. It is therefore of interest that in the K1 inclusion, the three melilite points (Fig. 6a) plot much higher than the spinel point. Although the Δ^{17}O of the lowest melilite point is -20‰, the same as Clayton and coworkers reported in refractory inclusions and their unaltered minerals (e.g., spinel), the Δ^{17}O of our spinel point is -28‰, 8‰ lower. However, it is also important to note that the Δ^{17}O value of the highest melilite point, -13‰, is still much lower than the typical melilite values of ≈ -3 to -5‰ reported by Mayeda et al. (1986), Clayton et al. (1977) and Young and Russell (1998) in CV Allende (Fig. 1).

Although Kainsaz inclusion K2 does not show as much alteration effects as K1, two of the three melilite points also fall outside the tight cluster formed by our spinel and diopside analyses just discussed (Fig. 6b). The highest melilite has a Δ^{17}O value of -14‰, similar to the two high values in inclusion K1. The next highest melilite point has a relatively high δ^{18}O but a much lower Δ^{17}O value, -23‰; a minor fraction of the area under this spot may have sampled diopside. In terms of

Table 1. Phase Compositions in Kainsaz, Ornans, and Colony Inclusions.

Inclusion-spot	Phase†	Na_2O	MgO	Al_2O_3	SiO_2	CaO	TiO_2	Cr_2O	FeO	Total	Ak
K1-01	mel + crack	<0.02	0.44	34.4	21.6	42.4	0.06	<0.01	0.41	99.3	3
K1-02	mel	<0.02	0.14	35.5	22.0	42.0	0.08	0.01	0.37	100.0	2
K1-03	sp	0.02	20.7	66.7	0.05	0.18	0.10	0.10	10.7	98.6	
K1-04	mel	0.04	0.57	33.8	22.3	42.3	<0.01	<0.01	0.27	99.3	6
K2-01	mel	0.08	1.10	32.6	23.3	42.5	0.07	<0.01	0.25	100.1	9
K2-02*	mel95%	0.13	1.49	32.7	24.8	42.0	0.02	<0.01	0.24	101.4	12
K2-03	sp	0.02	27.6	69.6	0.01	0.09	0.38	0.12	1.01	98.8	
K2-04	di	0.02	17.4	3.1	53.5	26.7	1.01	0.11	0.19	102.0	
K2-05	di	0.02	17.2	3.6	52.93.	26.2	1.02	0.11	0.22	101.3	
K2-06	an80%	0.14	0.25	35.1	41.9	20.9	0.21	<0.01	0.03	98.5	
K2-06	mel20%	0.20	0.90	33.5	23.4	41.7	0.14	<0.01	0.12	99.9	8
K2-07	di	0.04	17.5	1.2	54.1	26.4	0.25	0.06	0.13	99.8	
K2-08	mel	0.04	0.11	35.2	21.5	42.4	0.19	0.09	0.13	99.7	2
O3-01	mel	0.22	1.02	33.1	23.5	40.7	0.03	<0.01	0.45	99.1	9
O3-02	di	0.12	18.1	3.4	52.5	24.8	0.62	0.03	0.27	100.4	
O3-03	mel	0.09	1.4	32.6	24.0	41.8	0.06	<0.01	0.13	100.1	11
O4-01	mel50%	0.48	1.97	31.1	26.3	40.0	0.03	<0.01	0.86	100.8	18
O4-01	px50%	0.09	18.0	3.10	54.8	25.6	0.23	0.04	0.36	102.3	
O4-02	mel	0.21	1.57	31.4	24.5	41.1	0.03	<0.01	0.59	99.5	14
O4-03*	px50%	0.07	15.4	8.7	49.5	25.3	0.09	0.15	0.62	99.9	
O5-01*	sp50%	0.06	18.2	63.6	0.07	0.04	0.55	0.04	19.1	100.2	
O5-02*	mel60%	0.06	0.65	38.2	21.5	38.9	0.11	<0.01	0.37	99.8	2
O5-03	mel	0.15	0.72	34.3	23.4	41.3	0.04	0.07	0.68	100.7	7
O5-04	mel	0.27	0.96	33.9	24.1	41.5	0.03	<0.01	0.58	101.4	9
O5-05	sp	0.03	16.7	69.5	0.33	0.28	0.20	0.10	14.2	101.5	
O5-06	mel	0.05	0.41	36.7	21.3	40.9	0.15	<0.01	0.37	100.0	1
O5-07	mel	0.15	0.74	34.1	23.2	41.4	0.04	<0.01	0.31	100.1	7
C1-01	mel	0.02	1.1	32.9	23.3	41.9	<0.01	<0.01	0.24	99.4	9
C1-02	sp	0.02	28.2	69.6	0.60	0.13	0.10	0.19	0.25	99.2	
C1-03	mel	0.05	2.8	30.7	23.9	39.3	0.04	0.08	0.30	97.4	14
C1-04	85%di	0.05	17.8	3.3	53.3	24.7	0.44	0.013	1.40	100.9	
C1-04	15%gl	0.23	1.4	19.8	52.5	2.9	0.06	<0.01	0.23	77.1	
C1-05*	80% di	0.31	12.7	12.4	44.2	24.5	2.23	0.24	0.43	97.2	
C1-06*	50% di	<0.02	11.7	17.5	41.4	25.2	4.01	0.20	0.28	100.3	
C1-07	mel	<0.02	2.6	29.0	25.8	41.8	<0.01	<0.01	0.12	99.4	20
C1-07	di	<0.02	12.3	13.5	45.4	24.6	2.54	0.05	2.26	100.6	

* The other material in the ion-probe crater is diopside in K2-02, fine-grained secondary minerals in O4-03, fine-grained secondary minerals in O5-01, spinel in O5-02, matrix in C1-05, and matrix in C1-06.

† Phase abbreviations: an; anorthite, di; diopside, gl; glass, mel; melilite, px; pyroxene, sp; spine.

Table 2. Melilite Compositions in Kainsaz, Ornans, and Colony Inclusions.

Inclusion-spot	Phase*	Ak (mol. %)	FeO	$\delta^{18}O$ (‰)	$\delta^{17}O$ (‰)	$\Delta^{17}O$
K1-01	mel	3	0.41	−14.5 ± 1.3	−20.6 ± 2.0	−13.1
K1-02	mel	2	0.38	−29.9 ± 1.3	−36.1 ± 2.7	−20.5
K1-04	mel	6	0.27	−23.1 ± 1.0	−26.9 ± 2.7	−14.9
K2-01	mel	9	0.35	−23.7 ± 1.1	−26.4 ± 2.3	−14.1
K2-02	mel, di	12	0.25	−34.5 ± 1.1	−41.1 ± 3.0	−23.2
K2-08	mel	2	0.13	−45.6 ± 1.6	−51.9 ± 2.2	−28.2
O3-01a	mel	9	0.45	−32.7 ± 1.1	−35.5 ± 2.3	−18.5
O3-01b	mel	9	0.45	−32.5 ± 2.4	−37.2 ± 1.1	−20.3
O3-03	mel	11	0.13	−32.4 ± 1.3	−34.3 ± 2.3	−17.5
O4-02	mel	14	0.59	−13.2 ± 1.3	−20.2 ± 2.6	−13.3
O5-01	mel	2	0.37	−13.2 ± 1.1	−16.4 ± 2.3	−9.5
O5-03	mel	7	0.68	−3.9 ± 1.3	−4.4 ± 2.6	−2.4
O5-04	mel	9	0.54	−14.7 ± 1.1	−16.6 ± 2.5	−9.0
O5-07	mel	1	0.31	−43.3 ± 1.1	−47.9 ± 2.4	−25.4
O5-06	mel, sp	7	0.36	−39.7 ± 1.3	−40.7 ± 2.3	−20.1
C1-01	mel	9	0.24	−41.9 ± 1.1	−47.6 ± 2.5	−25.9
C1-03	mel	14	0.30	−50.7 ± 1.2	−54.7 ± 2.1	−28.4
C1-07	mel, di	20	0.12	−50.5 ± 1.0	−53.2 ± 2.4	−26.9

* Phase abbreviations: di; diopside, mel; melilite, sp; spinel.

Table 3. Compositions of spinel, diopside, and other phases in Kainsaz, Ornans, and Colony Inclusions.

Inclusion-spot	Phase*	FeO	δ^{18}O (‰)	δ^{17}O (‰	Δ^{17}O
K1-03	sp	10.7	−54.7 ± 1.1	−56.7 ± 2.1	−28.3
K2-03	sp	1.01	−51.7 ± 1.4	−48.7 ± 3.0	−21.8
K2-04	di	0.19	−44.3 ± 1.4	−51.0 ± 2.1	−28.0
K2-05	di		−44.0 ± 1.4	−53.3 ± 2.5	−30.4
K2-06	an, mel, s		−45.7 ± 1.6	−45.2 ± 2.8	−21.5
K2-07	di	0.13	−46.9 ± 2.3	−49.6 ± 2.9	−25.3
O3-02	di	0.27	−41.9 ± 1.1	−42.6 ± 2.4	−20.8
O4-01	px, mel	0.36	−30.2 ± 1.4	−34.9 ± 2.2	−19.2
O4-03	px	0.62	−38.5 ± 1.2	−43.5 ± 2.0	−23.5
O5-02	sp, mel		−44.4 ± 1.0	−47.9 ± 2.2	−24.8
O5-05	sp	14.2	−49.9 ± 1.1	−54.2 ± 2.3	−28.3
C1-02	sp	0.25	−49.2 ± 1.2	−55.9 ± 2.2	−30.3
C1-04	gls		−3.4 ± 1.5	−5.3 ± 3.1	−3.5
C1-05	di, mx	0.43	−17.2 ± 1.8	−20.4 ± 4.6	−11.5
C1-06	di, mx	0.28	−12.1 ± 1.2	−22.1 ± 2.9	−15.8

* Phase abbreviations: an; anorthite, di; diopside, gl; glass, mx; matrix, mel; melilite, px; pyroxene, sp; spinel.

Δ^{17}O, it is a member of the diopside-spinel cluster, but the uncertainty in δ^{18}O is relatively large. The third melilite point plots in this cluster both in terms of Δ^{17}O and in terms of δ^{18}O, and a point that sampled both melilite and anorthite (the one other phase that Clayton et al., 1977, commonly found to have high Δ^{17}O values similar to those of melilite) is a member of the cluster with Δ^{17}O about the same as that of the spinel, −22‰.

Our data for the three melilite-bearing inclusions in Ornans are shown in Figures 6c–6e. In O3 (Fig. 6c), we were unable to find spinel large enough to analyze, but the composition of the diopside is in the primitive field; Δ^{17}O is −20.8‰. The three melilite points (Fig. 6c, Table 2) showed a remarkable uniformity with Δ^{17}O values in the−range from −17.5‰ to −20.3‰. Thus, these values are only slightly displaced from the primitive composition, consistent with our petrographic evidence that O3 was the least altered of the three inclusions from Ornans.

In inclusion O4 (Fig. 6d), the spinels were again too small to analyze, but we obtained data for one diopside (O4-03), with minimal overlap onto secondary minerals, and the modal composition of O4-01 was around 50% diopside and 50% melilite. The diopside plus secondary minerals point fell in the primitive range (Δ^{17}O = −23.5‰) and the diopside + melilite point fell just above this range at −19.2‰. We obtained one point on pure melilite with Δ^{17}O of −13.3‰. If we use this melilite composition to make a rough correction of the mixed diopside–melilite point, the resulting diopside Δ^{17}O value is <−21‰.

In the O5 inclusion, we were able to measure spinel with the expected primitive (−21‰ or lower) compositions (Fig. 6e) but observed a wide range of melilite compositions. In our highest melilite point (O5-03), Δ^{17}O is only −2.4‰, a value similar to that observed in matrix. At the other extreme is a primitive melilite (O5-07), having Δ^{17}O = −25‰.

All four points obtained for pure phases in Colony inclusion C1 have similar Δ^{17}O values; the range is from −26‰ to −30‰ (Fig. 6f). As discussed above, three other points listed in Table 1 (and Table 3) sampled glass or mixtures of phases. Point 4 seems to have sampled diopside and Al-rich glass, but analytical totals were always low, perhaps because there was a crack near the analyzed point; both points 5 and 6 sampled a mixture of diopside and matrix.

In an independent study carried out on the same ion probe, Itoh et al. (2000) analyzed melilite in two refractory inclusions

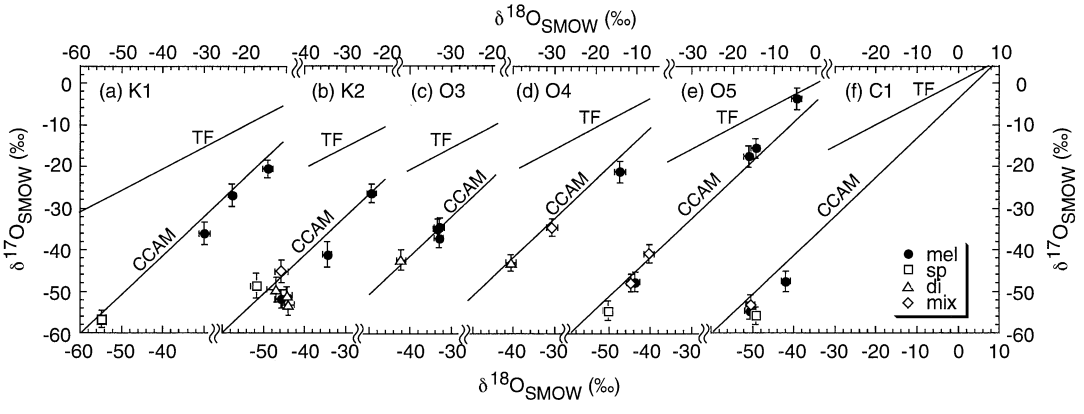

Fig. 6. Oxygen isotope data for phases in the six refractory inclusions: (a) Kainsaz K1, (b) Kainsaz K2, (c) Ornans O3, (d) Ornans O4, (e) Ornans O5, and (f) Colony C1.

in CO3.0 Yamato 81020. Their melilite analyses were similar to our Colony observations. In the two inclusions they analyzed, the $\Delta^{17}O$ values in the melilite were less than −22‰. Also, Yurimoto et al. (2001) have recently discovered a large (200-μm) igneous melilite grain wrapped around a hibonite–spinel refractory inclusion in which $\Delta^{17}O$ in the large melilite is ≈−6‰, but that in the core (Åk <0.1%) has $\Delta^{17}O \approx -25$‰. This inclusion seems to be an atypical case requiring an unusual formation process including two high-temperature (>1300 K) stages. Because no similar inclusions have been reported in the past, it may be a rare type.

Thus, there is good reason to believe that melilite having $\Delta^{17}O \leq -25$‰ is typical of refractory inclusions in CO3.0 chondrites. Because the only difference between type 3.0 CO chondrites and those of higher subtype appears to be the degree of aqueous/metamorphic alteration (e.g., Scott and Jones, 1990; Kojima et al., 1995), we conclude that the melilite originally formed in the nebula had $\Delta^{17}O$ values near −25‰ or lower and that the much higher values commonly observed in melilite in the higher subtypes were produced during alteration. Because volume diffusion is unable to transport O to the centers of melilite grains while leaving the mafic minerals unequilibrated in FeO/(FeO + MgO), we suggest that the melilite alteration required another mechanism, probably one associated with aqueous alteration.

If the oxygen-isotopic composition of melilite is affected by aqueous/metamorphic processes, then these measurements may provide a sensitive indicator of petrologic subtype. The three CO3 meteorites we analyzed showing differing degrees of alteration, increasing in the order: Colony, Kainsaz, Ornans. Colony exhibits pristine isotopic values. Because the biggest change in oxygen isotope systematics is observed between Colony and Kainsaz, our inferred petrologic subtypes are Colony (3.0), Kainsaz (3.2), and Ornans (3.3).

4.2. Scenario for Melilite Formation during Aqueous Alteration

Aqueous/metamorphic alteration effects are common in the high-petrographic subtypes of CO chondrites. These commonly involve the replacement of melilite by a fine-grained mix of nepheline, anorthite, and other phases such as andradite and hedenbergite (Kojima et al., 1995; Russell et al., 1998). As noted above, most (but not all) researchers agree that the site of this alteration was within the asteroidal parent body. An example of a nebular alteration scenario for CV chondrites is discussed by Ikeda and Kimura (1995).

Thus, the key question is, what circumstances could lead to the formation of new melilite in which the nebular O has been replaced? We suggest that in slightly altered systems such as low type-3 chondrites, the composition of the microenvironment is responsible for the set of phases produced by the action of H_2O and that an aqueous phase having low Mg, Si and Na concentrations may allow melilite to dissolve and immediately reprecipitate. The ideal conditions for O-isotope replacement obtain if melilite dissolved and reprecipitated in the presence of a film of H_2O.

What circumstances would cause melilite to dissolve and reprecipitate? The obvious answer is that the original material was in a higher energy state, either because of small grain size or crystalline defects. We suggest three possibilities: (1) that, following a nebular melting event, spinel crystallized but the melilite-rich mesostasis chilled to a fine-grained, cryptocrystalline material; (2) impact processes, perhaps during the compaction of the parent body, crushed the nebular melilite to a fine grain size and introduced defects into the crystals; or (3) melilite originated in the nebula as aggregates of fine grains that experienced only a minor degree of melting during the formation of the inclusions. Both of these would result in crystalline energy states higher than those in coarse melilite.

The transport of H_2O along grain surfaces should be much more rapid than that of Mg, Fe, Na, or Si because of the faster diffusion of uncharged H_2O molecules through cracks compared with ions (which would migrate via ion exchange) and the much higher concentration of H_2O compared with the ionic species. It thus seems plausible that, during aqueous alteration processes on the asteroid, much of the O present at grain boundaries could be from a pervasive aqueous phase while leaving the cationic isotopic compositions of the new melilite dominated by the ions liberated from the dissolving melilite.

This scenario leads to the prediction that other fine-grained phases should also experience aqueous alteration. We know that anorthite is commonly altered, but why might this process have less effect on spinel, diopside, and much of the olivine? The speculative answer is that following the compaction of the parent body (necessary to allow the transport of small quantities of liquid H_2O and thus the onset of aqueous alteration), the latter phases were less reactive, perhaps because they were less damaged during the compaction process.

4.3. Relationship between $\Delta^{17}O$ and the Chemical Composition of the Melilite

In part to test the above ideas, we plotted melilite $\Delta^{17}O$ vs. compositional parameters that might be associated with alteration.

In Figure 7a, a plot of $\Delta^{17}O$ vs. the FeO content of the melilite, we observe a positive trend ($R^2 = 0.56$). This is consistent with the view that both of these parameters tend to increase with increasing degree of (asteroidal aqueous) alteration. A similar but appreciably weaker positive trend is found between $\Delta^{17}O$ and Na_2O ($R^2 = 0.20$).

In contrast, no correlation is observed on the plot of melilite $\Delta^{17}O$ vs. the Åk content of the melilite (Fig. 7b). A positive trend would be expected if the nebular phase was nearly pure (<10 mol. % Åk) gehlenite and akermanite was mainly produced during asteroidal alteration processes. The absence of such a trend (and the wide range in CO3.0 Colony in particular) suggests that nebular melilite had a wide range (0 to 20 mol. %) of Åk contents (consistent with the crystallization of nebular melts or, possibly, by fractional condensation), and that any change produced during the alteration of CO chondrites of petrologic type ≤3.3 is minor by comparison.

We also plotted (but do not show) melilite FeO vs. the Åk content. As expected, these parameters are not correlated because Åk zonation is a primary characteristic of melilite, whereas it is plausible that FeO was introduced during alteration.

Returning to Figure 7a, we note that the scatter both in $\Delta^{17}O$ and in FeO increase with increasing petrographic subtype

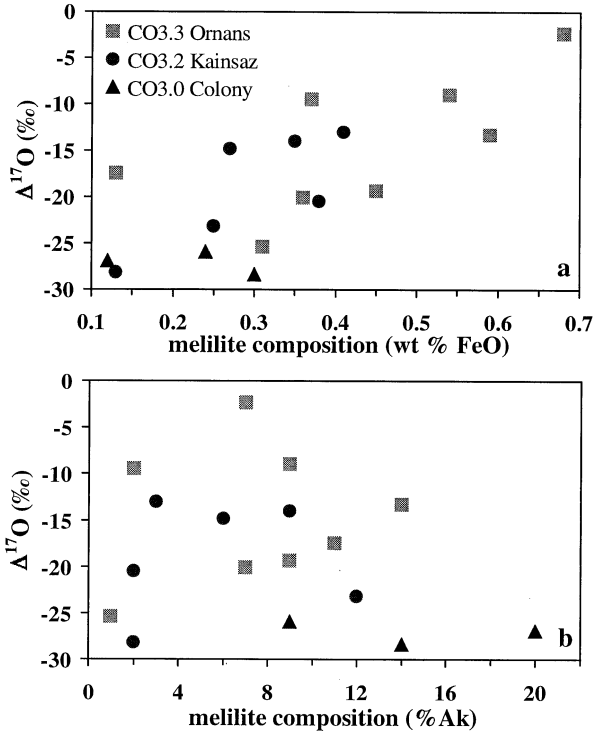

Fig. 7. Melilite $\Delta^{17}O$ values are plotted against two compositional parameters, FeO content, and akermanite content. (a) A correlation is observed between $\Delta^{17}O$ and FeO content of the melilite. As discussed in more detail in the text, we suggest that both parameters increase with increasing degree of aqueous alteration. If one anomalously high Colony point is neglected, the mean content and the standard deviation of both parameters increase through the subtype sequence from 3.0 to 3.3. (b) No correlation is observed between $\Delta^{17}O$ and the Åk content. We interpret this to mean that the Åk contents were largely established in the solar nebula.

through the sequence 3.0 to 3.3. This suggests that the mean FeO content and the relative standard deviation of the FeO content of melilite could be used as parameters for assigning subtypes within this subtype range.

4.4. Aqueous Alteration, the CCAM line, and the Bulk O-Isotopic Composition of Chondrites

If the alteration of melilite from $\Delta^{17}O \leq -20‰$ to higher values is the result of aqueous alteration, a plausible hypothesis is that all the CAI minerals that plot along the CCAM line at $\Delta^{17}O > -20‰$ were altered by exchange of O with H_2O and with other loosely bound O in the matrix. This suggests that caution is necessary when attempting to use data on such minerals to constrain processes that occurred in the nebula or still earlier.

Whether this alteration of the fine-grained inclusions that we and Itoh et al. (2000) studied in CO3.0 chondrites can be extrapolated to coarse-grained (e.g., type-B) refractory inclusions is unresolved. Yurimoto et al. (1998) argued that the best way to understand high $\Delta^{17}O$ values in such inclusions is to invoke a second melting event, but scenarios involving asteroidal aqueous alteration should also be investigated in more detail.

It has long been recognized that the mean $\Delta^{17}O$ varies among the carbonaceous chondrites. In particular, Clayton and Mayeda (1999) have interpreted the observed range in terms of a model involving variable amount of water and rock. As discussed above, the effect of aqueous alteration has been to change the O-isotopic compositions of some minerals in refractory inclusions from $\Delta^{17}O$ values $< -20‰$ to much higher values. The evidence suggests that the primordial (before aqueous alteration) oxygen-isotopic compositions of refractory inclusions may have been essentially the same in all carbonaceous chondrite groups and raises the possibility that $\delta^{17}O$-$\delta^{18}O$ arrays based on the phases of refractory inclusions (commonly with slopes ≈ 0.9) are mainly the result of aqueous alteration. Note that we are not suggesting the chondrule array with a higher slope near 1.0 was produced in a similar way; there is no evidence to suggest that the major chondrule minerals in relatively unaltered chondrites such as Colony and Y81020 did not retain their original nebular compositions.

This leads to the interesting suggestion that, at least for carbonaceous chondrites, the whole-rock $\Delta^{17}O$ value might increase with increasing degree of aqueous alteration (this scenario includes the assumption that any excess H_2O was subsequently lost). The fraction of matrix (which has largely equilibrated with the nebular gas) will also have played a role, thus it would be difficult to use $\Delta^{17}O$ as a measure of the relative degree of intergroup aqueous alteration.

Some support for this idea can be found in the data of Clayton and Mayeda (1999) for the oxidized and reduced subgroups of CV chondrites. After removal of ungrouped Ningqiang from their oxidized CV list, we find that the mean $\Delta^{17}O$ of the less-altered reduced subgroup ($n = 8$) $\approx -4.83 \pm 0.81‰$, whereas that for the more altered oxidized subgroup ($n = 6$) is $\approx -3.54 \pm 0.86‰$; application of the *t*-test shows that this difference is significant at the 98% confidence level. However, Clayton and Mayeda's data also show considerable scatter between replicates of individual meteorites; thus, it would be difficult to use a single whole-rock O-isotopic composition as the basis of a firm conclusion regarding degree of aqueous alteration.

5. SUMMARY

Our melilite results are summarized on a three-isotope diagram in Figure 8. In addition to the TF line reference lines are drawn at $\Delta^{17}O = -5‰$, the lower limit of the four melilite compositions of mechanically separated samples studied by Clayton and coworkers, and at $\Delta^{17}O = -21‰$, a rough upper bound on the $\Delta^{17}O$ values of phases in unaltered refractory inclusions. With one exception, our melilite $\Delta^{17}O$ values are lower that those obtained by Clayton and coworkers in CV3 Allende. Our melilite data for CO3.0 Colony, like those obtained for melilite in CO3.0 Yamato 81020 by Itoh et al. (2000), are primitive, similar in $\Delta^{17}O$ to the spinel in the same inclusions. Two of our CO3.2 Kainsaz melilites preserve primitive compositions, as does one of the set from CO3.3 Ornans. The remaining Kainsaz and Ornans melilites form a linear trend extending from the compositions of primitive refractory inclusions to the compositions observed in Allende.

We interpret the differences between melilites from type-3.0 CO chondrites and those of higher subtype to be the result of

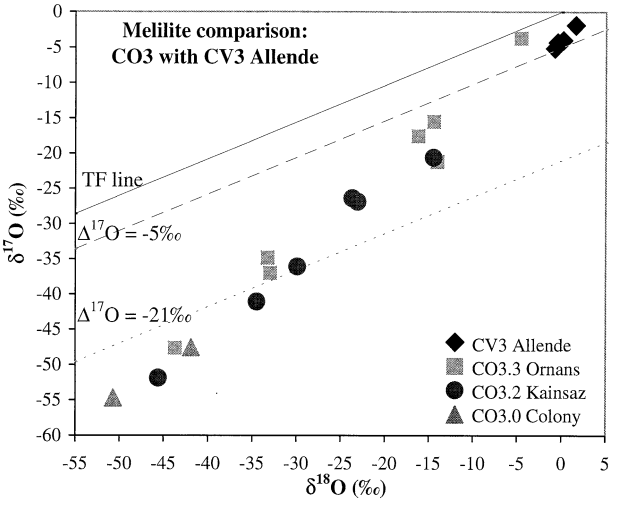

Fig. 8. Oxygen-isotope data for melilite in CO3 chondrites (this study) and for CV3 Allende (data repeated from Fig. 1. The Allende data are all above $\Delta^{17}O = -5‰$, whereas all CO3.0 Colony data have $\Delta^{17}O$ lower than $-21‰$. With the exception of one high Ornans value, $\Delta^{17}O$ values in melilite in CO3.2 Kainsaz and CO3.3 Ornans scatter between these extremes.

more extensive asteroidal alteration in the higher subtypes, by aqueous processes, thermal metamorphism, or both. We suggest that the CO3.0 chondrites are the carbonaceous chondrites that experienced the least amount of aqueous alteration or thermal metamorphism. It follows that the low ($\leq -21‰$) melilite $\Delta^{17}O$ values common in these chondrites preserve primitive nebular compositions and that the less negative melilite $\Delta^{17}O$ values observed in some other carbonaceous chondrites may also reflect aqueous alteration processes.

Acknowledgments—We are grateful to A. Krot, H. Palme, and an anonymous referee for constructive reviews. Technical assistance was provided by Sydney Zhang and Subin Yoo. This research was supported by Kagaku Gijutsu-cho, Monbu-sho, and by National Science Foundation grant EAR-9805229. JTW acknowledges fellowship support from the Japanese Society for the Promotion of Science.

Associate Editor: H. Palme

REFERENCES

Blander M. and Fuchs L. H. (1975) Calcium-aluminum-rich inclusion in the Allende meteorite; evidence for a liquid origin. *Geochim. Cosmochim. Acta* **39,** 1605–1619.

Blum J. D., Wasserburg G. J., Hutcheon I. D., Beckett J. R., and Stolper E. M. (1989) Origin of opaque assemblages in CV3 meteorites: Implications for nebular and planetary processes. *Geochim. Cosmochim. Acta* **53,** 543–556.

Brearley A. J., Bajt S., and Sutton S. R. (1995) Distribution of moderately volatile trace elements in fine-grained chondrule rims in the unequilibrated CO3 chondrite, ALH A77307. *Geochim. Cosmochim. Acta* **59,** 4307–4316.

Cassen P. (1996) Models for the fractionation of moderately volatile elements in the solar nebula. *Meteorit. Planet. Sci.* **31,** 793–806.

Choi B.-G., Krot A. N., and Wasson J. T. (2000) Oxygen-isotopes in magnetite and fayalite in CV chondrites Kaba and Mokoia. *Meteorit. Planet. Sci.* **35,** 1239–1248.

Choi B.-G., McKeegan K. D., Leshin L. A., and Wasson J. T. (1997) Origin of magnetite in oxidized CV chondrites: In situ measurement of oxygen isotope compositions of magnetite and olivine in CV3 Allende. *Earth Planet. Sci. Lett.* **146,** 337–349.

Chou C.-L., Baedecker P. A., Chou C.-L., Robinson K. L., and Wasson J. T. (1976) Allende inclusions: Volatile-element distribution and evidence for incomplete volatilization of presolar solids. *Geochim. Cosmochim. Acta* **40,** 85–94.

Clayton R. N., Grossman L., and Mayeda T. K. (1973) A component of primitive nuclear composition in carbonaceous meteorites. *Science* **182,** 485–488.

Clayton R. N. and Mayeda T. K. (1984) The oxygen isotope record in Murchison and other carbonaceous chondrites. *Earth Planet. Sci. Lett.* **67,** 151–161.

Clayton R. N. and Mayeda T. K. (1999) Oxygen isotope studies of carbonaceous chondrites. *Geochim. Cosmochim. Acta* **63,** 2089–2104.

Clayton R. N., Mayeda T. K., Goswami J. N., and Olsen E. J. (1991) Oxygen isotope studies of ordinary chondrites. *Geochim. Cosmochim. Acta* **55,** 2317–2337.

Clayton R. N., Onuma N., Grossman L., and Mayeda T. K. (1977) Distribution of the presolar component in Allende and other carbonaceous chondrites. *Earth Planet. Sci. Lett.* **34,** 209–224.

Grossman J. N. and Rubin A. E. (1999) The metamorphic evolution of matrix and opaque minerals in CO chondrites (abstract). *Lunar Planet. Sci.* **30,** 1639–1640.

Grossman L. (1972) Condensation in the primitive solar nebula. *Geochim. Cosmochim. Acta* **36,** 597–619.

Hiyagon H. and Hashimoto A. (1999) ^{16}O excesses in olivine inclusions in Yamato-86009 and Murchison chondrites and their relation to CAIs. *Science* **283,** 828–831.

Ikeda Y. and Kimura M. (1995) Anhydrous alteration of allende chondrules in the solar nebula I: Description and alteration of chondrules with known oxygen-isotopic compositions. *Proc. NIPR Symp. Antarct. Meteorites* **8,** 97–122.

Itoh S., Kojima H., and Yurimoto H. (2000) Petrography and oxygen isotope chemistry of calcium-aluminum rich inclusions in CO chondrites [abstract]. *Lunar Planet. Sci.* **31,** abs.1323.

Kallemeyn G. W. and Wasson J. T. (1982) The compositional classification of chondrites-III. Ungrouped carbonaceous chondrites. *Geochim. Cosmochim. Acta* **46,** 2217–2228.

Kojima T., Yada S., and Tomeoka K. (1995) Ca-Al-rich inclusions in three Antarctic CO3 chondrites, Yamato-81020, and Yamato-790992: Record of low-temperature alteration. *Proc. NIPR Symp. Antarct. Meteorites* **8,** 79–96.

Krot A. N., Scott E. R. D., and Zolensky M. E. (1995) Mineralogical and chemical modification of components in CV3 chondrites: Nebular or asteroidal processing? *Meteoritics.* **30,** 748–775.

Mayeda T. K., Clayton R. N., and Nagasawa H. (1986) Oxygen isotope variations within Allende refractory inclusions [abstract]. *Lunar Planet. Sci.* **17,** 526–527.

Meeker G. P. (1983) Replacement textures in CAI and implications regarding planetary metamorphism. *Geochim. Cosmochim. Acta* **47,** 707–721.

Rubin A. E., James J. A., Keck B. D., Weeks K. S., Sears D. W. G., and Jarosewich E. (1985) The Colony meteorite and variations in CO3 chondrite properties. *Meteoritics* **20,** 175–196.

Russell S. S., Huss G. R., Fahey A. J., Greenwood R. C., Hutchison R., and Wasserburg G. J. (1998) An isotopic and petrologic study of calcium-aluminum-rich inclusions from CO3 meteorites. *Geochim. Cosmochim. Acta* **62,** 689–714.

Ryerson F. J. and McKeegan K. D. (1994) Determination of oxygen self-diffusion in åkermanite, anorthite, diopside, and spinel: Implications for oxygen isotopic anomalies and the thermal histories of Ca-Al-rich inclusions. *Geochim. Cosmochim. Acta* **58,** 3713–3734.

Sakai T. and Yurimoto H. (1999) Oxygen isotope distribution in CAIs of the Murchison meteorite [abstract]. *Lunar Planet. Sci.* **30,** abs.1528.

Scott E. R. D. and Jones R. H. (1990) Disentangling nebular and asteroidal features of CO3 carbonaceous chondrite meteorites. *Geochim. Cosmochim. Acta* **54,** 2485–2502.

Sears D. W. G., Batchelor D., Lu J., and Keck B. D. (1991) Metamorphism of CO and CO-like chondrites and comparisons with type 3 ordinary chondrites. *Proc. NIPR Symp. Antarct. Meteorites* **4,** 319–343.

Shibata Y. (1996) Opaque minerals in Antarctic CO3 carbonaceous

chondrites, Yamato-74135, −790992, −791717, −81025, −82050. *Proc. NIPR Symp. Antarct. Met.* **9,** 79–96.

Stolper E. and Paque J. M. (1986) Crystallization sequences of Ca-Al-rich inclusions from Allende: The effects of cooling rate and maximum temperature. *Geochim. Cosmochim. Acta* **50,** 1785–1806.

Wasson J. T. (2000). Oxygen-isotopic evolution of the solar nebula. *Rev. Geophys.* **38,** 491–512.

Young E. D. and Russell S. S. (1998) Oxygen reservoirs in the early solar nebula inferred from an Allende CAI. *Science* **282,** 452–455.

Yurimoto H., Ito M., and Nagasawa H. (1998) Oxygen isotope exchange between refractory inclusion in Allende and solar nebula gas. *Science* **282,** 1874–1877.

Yurimoto H., Morioka M., and Nagasawa H. (1989) Diffusion in single crystals of melilite: I. Oxygen. *Geochim. Cosmochim. Acta* **53,** 2387–2394.

Yurimoto H., Rubin A. E., Itoh S., and Wasson J. T. (2001) Non-stoichiometric Al-rich spinel in an ultra-refractory inclusion from CO chondrite [abstract]. *Lunar Planet. Sci.* **32,** abs. 1557.pdf.